PHYSICAL REVIEW B VOLUME 44, NUMBER 19 15 NOVEMBER 1991-I

Quantum confinement of excitons in the spin-orbit-split-off band in ZnSe/ZnS strained-layer superlattices

Sadao Adachi
Department of Electronic Engineering, Faculty of Engineering, Gunma University, Kiryu-shi, Gunma 376, Japan

Tsunemasa Taguchi
Department of Electrical Engineering, Faculty of Engineering, Osaka University, Suita-shi, Osaka 565, Japan
(Received 21 May 1991; revised manuscript received 23 July 1991)

We report the observation of two-dimensional (2D) electronic states confined in the spin-orbit-split-off band in ZnSe/ZnS strained-layer superlattices. The steplike absorption edge at the $E_0+\Delta_0$ gap and the corresponding 2D exciton peak have been clearly identified in spectroscopic-ellipsometry spectra. The 2D-exciton Rydberg energy obtained is about 160 meV, which is considerably larger than that at the $E_0+\Delta_0$ gap of bulk ZnSe ($\sim$40 meV). Calculated steplike-edge energies using the model-solid approach and the Kronig-Penney model agree well with the experimental observations.

I. INTRODUCTION

Many experimental and theoretical studies have been reported on the electronic and optical properties of semiconductor quantum wells and superlattices.[1] Some of the III-V and II-VI compounds, and in particular ZnSe, form crystals with the zinc-blende structure (T_d point-group symmetry). The zinc-blende crystal has three degenerate valence bands at Γ (Γ_{15}^v). These bands are strictly degenerate only in the absence of strain and spin-orbit splitting. They are labeled here by hh (heavy-hole band: $J=\frac{3}{2}$ and $m_j=\pm\frac{3}{2}$), lh (light-hole band: $J=\frac{3}{2}$ and $m_j=\pm\frac{1}{2}$), and so (spin-orbit-split-off band: $J=\frac{1}{2}$ and $m_j=\pm\frac{1}{2}$). When no strain is present, spin-orbit interaction splits the Γ_{15}^v valence band into the Γ_8^v bands (hh and lh) and the Γ_7^v band (so). The corresponding splitting energy is labeled by Δ_0. Shear components of the strain lead to additional splittings, which interact with the spin-orbit splittings to produce the final valence-band positions. There are many studies of the quantum-confinement and/or strain effects on the hh- and lh-rated (quasi-) two-dimensional (2D) excitons and the corresponding steplike joint-density edges in III-V and II-VI semiconductor quantum-well structures.[2]

There have been, however, a very few reports on the hole confinement in the so band in multiple-quantum-well heterostructures.[3-5] Mendez *et al.*[3] reported the observation of transitions associated with the so-band holes in the electroreflectance spectra of GaAs/$Al_{1-x}Ga_xAs$ superlattices. They found that the experimental quantum-confinement energies compare very favorably with those calculated from the Kronig-Penney model. From the low-temperature ($\sim$8-K) photoluminescence excitation spectra, Duggan *et al.*[4] deduced the existence of the so-related quantum transitions in a number of GaAs/$Al_{1-x}Ga_xAs$ multiple-quantum-well samples. A sharp peak was seen at high energy (>1.9 eV), and the strength of this feature and the variation of its peak energy as a function of well width and aluminum fraction provided good evidence that the peak is associated with the electron–so-hole transition. Garriga *et al.*[5] studied the confinement and interlayer coupling effects on the optical interband transitions of GaAs/AlAs superlattices using spectroscopic ellipsometry. For some of the superlattices, they were also able to see an indication of the electron–so-hole transition ($E_0+\Delta_0$ gap). To our knowledge, however, no clear evidence of the hole confinement in the so band has been reported in II-VI semiconductor quantum-well heterostructures.

In this paper we report an experimental evidence of the so-band quantum confinement (i.e., the so-related 2D exciton and steplike joint-density edge) in ZnSe/ZnS strained-layer superlattices (SLS's). We used spectroscopic ellipsometry (SE) to study the effects of quantum confinement and strain on the band edges of both the well and barrier layers in ZnSe/ZnS SLS's. The so- and lh-related 2D excitons and the corresponding steplike joint-density edges have been clearly identified in the SE spectra. Theoretical calculations of the steplike-edge energies using the model-solid approach[6,7] and the Kronig-Penney model were also performed and are found to agree well with the experimental observations.

II. EXPERIMENT

The ZnSe/ZnS SLS's used in this study were grown by low-pressure metalorganic chemical vapor deposition on (100)-oriented GaAs substrates.[8] The SLS's consist of a ZnSe well layer (25 Å thick) and a ZnS barrier layer (50 Å thick) with a period of 150 cycles. We already reported that x-ray-diffraction and transmission-electron-microscopy analyses confirm the presence of high-quality SLS with this sample dimension.[9] SE data were obtained at room temperature using a commercial SOPRA rotating-polarizer instrument (model ES4G, Seika Corp.) with tracking analyzer over the photon-energy range 1.5–5.3 eV. Measurements were made after cleaning the sample surfaces with methanol. The angle of incidence was 75°.

III. RESULTS AND DISCUSSION

An advantage of ellipsometry is that the complex dielectric constant can be obtained without Kramers-Kronig analysis. In Fig. 1 we show the dielectric-function spectra $\epsilon(\omega)=\epsilon_1(\omega)+i\epsilon_2(\omega)$ of a ZnSe/ZnS SLS measured by SE. As seen in the figure, the SE data reveal clear structures at the 2.8–3.5-eV and 4.7–5.3-eV regions. These structures originate from transitions at the $E_0-(E_0+\Delta_0)$ and $E_1-(E_1+\Delta_1)$ edges. The low-energy part of the superlattice spectra (≤ 2.85 eV) is disturbed by the regular interference fringes. The E_1 and $E_1+\Delta_1$ energies measured here are ~ 4.85 and ~ 5.15 eV, respectively, which are ~ 0.1 eV larger than those obtained in the bulk ZnSe.[10]

Let us say special attention to the so-related interband transitions in the SLS. The $\epsilon(\omega)$ spectra are shown on an expanded energy scale in Fig. 2(b). For comparison, we also measured SE spectra in the $E_0-(E_0+\Delta_0)$ spectral region of bulk ZnSe. The bulk crystal used was grown by a recrystallization traveling-heater method and was single crystalline, not intentionally doped, and of high resistivity.[11] The results of this experiment are shown in Fig. 2(a).

The bulk-ZnSe SE data reveal clear structures at ~ 2.7 eV (E_0) and at ~ 3.1 eV ($E_0+\Delta_0$). The arrows at 2.89 and 3.19 eV in Fig. 2(b) represent the positions of the lh-e and so-e exciton peaks ($n=1$), respectively. The SLS SE data show distinct spectral features in the neighborhood of these excitonic regions. The interference background is suppressed in the derivative spectra shown in Fig. 3, and the positions of these components can be determined fairly accurately.

The contribution to $d\epsilon/dE$ ($E=\hbar\omega$) of the steplike joint-density edge is given by[12]

$$\frac{d\epsilon^{\alpha}(\omega)}{dE}=a_{\alpha}^{2D}\{\chi^{-3}\ln(1-x^2)+[\chi(1-x^2)]^{-1}\}\ , \quad (1)$$

with

$$\chi=(E+i\Gamma)/E_{s\alpha}^{2D}\ , \quad (2)$$

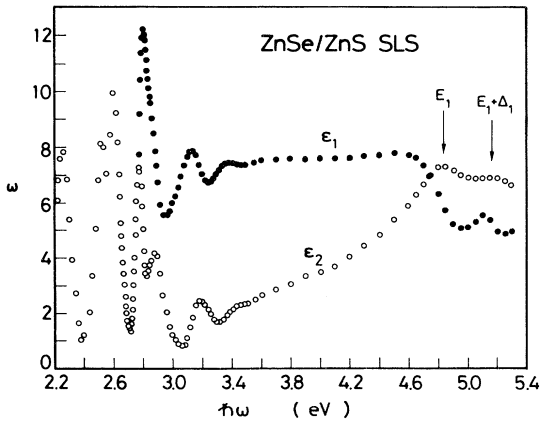

FIG. 1. Real (ϵ_1) and imaginary (ϵ_2) parts of the dielectric function of the ZnSe (25 Å)/ZnS (50 Å) SLS. They are obtained from ellipsometry measurement.

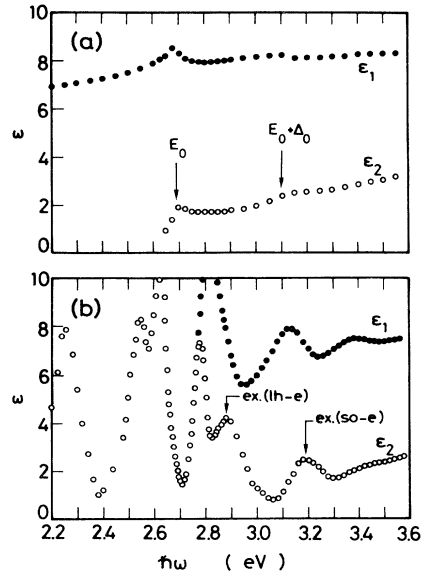

FIG. 2. Real (ϵ_1) and imaginary (ϵ_2) parts of the dielectric function of the (a) bulk-ZnSe and (b) ZnSe (25 Å)/ZnS (50 Å) SLS's.

where $E_{s\alpha}^{2D}$ is the steplike-edge energy [α stands for the hh-e (h), lh-e (l), or so-e (s) state], A_{α}^{2D} is the steplike-edge strength parameter, and Γ is a phenomenological damping energy. The contribution to $d\epsilon/dE$ of the 2D exciton is also written as

$$\frac{d\epsilon^{ax}(\omega)}{dE}=\frac{B_{\alpha}^{2D}}{[(E_{s\alpha}^{2D}-G_{\alpha}^{2D})-(E+i\Gamma)]^2}\ , \quad (3)$$

where G_{α}^{2D} is the 2D-exciton Rydberg energy and B_{α}^{2D} is

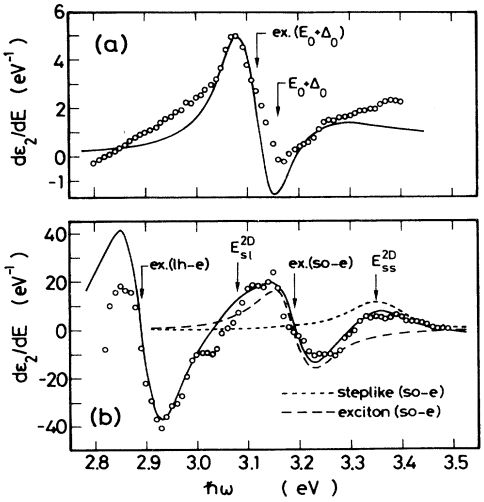

FIG. 3. Fits to the first derivatives of the imaginary parts of the dielectric function of the (a) bulk-ZnSe and (b) ZnSe (25 Å)/ZnS (50 Å) SLS's as a function of photon energy. Individual contributions of the so-e transitions are also shown in this figure [(b)] by the dotted [one-particle, Eq. (1)] and dashed lines [excitonic, Eq. (3)].

the exciton oscillator-strength parameter.

The open circles in Fig. 3(b) are first derivatives of the dielectric function $d\epsilon_2/dE$ numerically computed from the ellipsometric data in the lh-e and so-e transition region. The solid line is the best-fit result of Eqs. (1) and (3) (i.e., the sum of the imaginary parts of these expressions). The parameters determined are as follows: $E_{sl}^{2D}=3.08$ eV, $A_l^{2D}=0.13$ eV^{-1}, $B_l^{2D}=0.30$ eV, $G_l^{2D}=0.19$ eV, and $\Gamma=0.07$ eV for the lh-e transitions, and $E_{ss}^{2D}=3.35$ eV, $A_s^{2D}=0.13$ eV^{-1}, $B_s^{2D}=0.12$ eV; $G_s^{2D}=0.16$ eV, and $\Gamma=0.07$ eV for the so-e transitions. The fit is seen to be quite good except in the energy region below 2.87 eV, where the measured SE data are disturbed by the regular interference fringes. We also found that the real part of the first-derivative dielectric function $(d\epsilon_1/dE)$ can be fitted well with these numerical parameters.

We also carried out the first-derivative analysis of the bulk-ZnSe SE data to determine the $(E_0+\Delta_0)$-gap parameters [see Fig. 3(a)]. Numerical expressions used to fit to the SE data are

$$\frac{d\epsilon^{3D}}{dE}=-A_{so}^{3D}[2(E+i\Gamma)^{-3}(2\chi_0^{0.5}-\chi_+^{0.5}-\chi_-^{0.5}) +0.5(E+i\Gamma)^{-2}(x_+^{-0.5}-x_-^{-0.5})] , \quad (4)$$

with

$$\chi_0=e_0+\Delta_0 , \quad \chi_\pm=E_0+\Delta_0\pm(E+i\Gamma) , \quad (5)$$

for the one-particle transitions at the $E_0+\Delta_0$ gap [three-dimensional M_0 critical point],[12,13] and

$$\frac{d\epsilon^x(\omega)}{dE}=\frac{B_{so}^{3D}}{[(E_0+\Delta_0-G_{so}^{3D}])-(E+i\Gamma)]^2} , \quad (6)$$

for the 3D-excitonic transitions. In Eqs. (4)–(6), A_{so}^{3D} and B_{so}^{3D} are the one-particle and exciton strength parameters, respectively, and G_{so}^{3D} is the exciton Rydberg energy ($E_0+\Delta_0$ excitons). This fitting result is shown by the solid line in Fig. 3(a). The parameters determined are $E_0+\Delta_0=3.16$ eV, $G_{so}^{3D}=0.04$ eV, $A_{so}^{3D}=20$ eV$^{1.5}$, $B_{so}^{3D}=0.03$ eV, and $\Gamma=0.07$ eV.

The large tetragonal elastic strains in the SLS layers can produce marked effects on the electronic properties through the deformation-potential interactions.[7] The hydrostatic component of the strain causes shifts in the bulk energy levels of the layers, and the shear component causes splittings of certain degenerate valence-band levels. The energy levels of the SLS are therefore determined, including the strain modification of the well structure and quantum-size effects. We shall use here the model-solid approach of Van de Walle and Martin[6,7] to predict the energy levels at ZnSe/ZnS SLS interfaces. The lattice constants, bulk moduli, and energy-band parameters used in the calculation are taken from Refs. 7 and 14, except the band-gap energy E_0 and the valence-band offset ΔE_v^0 (the offset between the hh band in ZnSe and lh band in ZnS without strain). The E_0-gap energy used here is 2.69 eV (ZnSe), which corresponds to the room-temperature values,[10] and ΔE_v^0 is assumed to be 0.82 eV, which is the same as Harrison's value.[15]

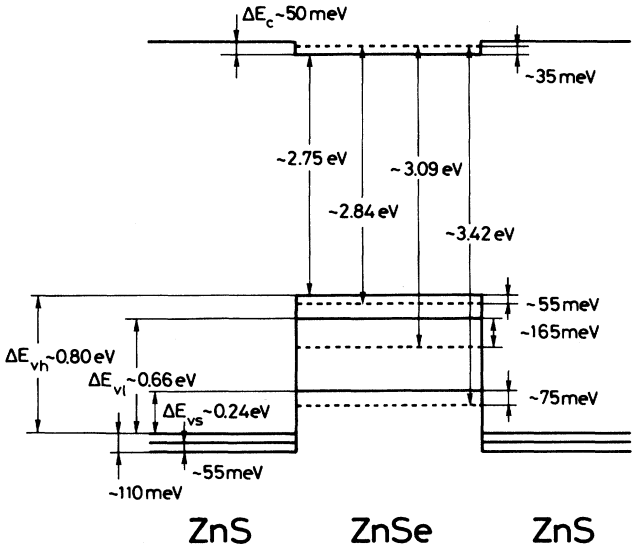

FIG. 4. Calculated band lineups and energy levels at a ZnSe (25 Å)/ZnS (50 Å) interface. The highest valence band in the ZnSe layer is the heavy-hole band, while that in ZnS is the light-hole band. The valence-band offsets are defined as the differences between the ZnSe and ZnS valence-band maxima: $\Delta E_{vh}=E_{hh}(\text{ZnSe})-E_{lh}(\text{ZnS})$, $\Delta E_{vl}=E_{lh}(\text{ZnSe})-E_{lh}(\text{ZnS})$, and $\Delta E_{vs}=E_{so}(\text{ZnSe})-E_{lh}(\text{ZnS})$. The dashed lines correspond to the energy positions of the $n=1$ electron (conduction band) and $n=1$ hole (three valence bands) quantum-confinement states.

We show in Fig. 4 the result of this calculation [a ZnSe (25 Å)/ZnS (50 Å) SLS]. It shows type-I quantum-well structure. In ZnSe the uppermost valence band is the hh band, while in ZnS it is the lh band. The lowest conduction band in ZnS is about 0.05 eV above that in ZnSe ($\Delta E_c\sim0.05$ eV). The conduction-band offsets ΔE_c in ZnSe/ZnS SLS's are always small. This prediction was confirmed by experimental observations.[14,16] The calculated energy differences between the conduction and valence bands in the ZnSe layer are ~2.75 eV (hh-e), ~2.89 eV (lh-e), and ~3.31 eV (so-e). It is noted that the increase in the lowest gap energy (~2.75 eV) is due to the effects of the biaxial compressive strains in the ZnSe layer. The final valence-band offsets are $\Delta E_{vh}=0.80$ eV $[E_{hh}(\text{ZnSe})-E_{lh}(\text{ZnS})]$, $\Delta E_{vl}=0.66$ eV $[E_{lh}(\text{ZnSe})-E_{lh}(\text{ZnS})]$, and $\Delta E_{vs}=0.24$ eV $[E_{so}(\text{ZnSe})-E_{lh}(\text{ZnS})]$.

The quantum-confinement energy levels for the electrons and holes in the ZnSe layer are calculated by means of the Kronig-Penney model with the above-mentioned band offsets and the following electron and hole effective masses:[17] $m_e/m_0=0.17$, $m_{hh}/m_0=0.78$, $m_{lh}=0.16$, and $m_{so}/m_0=0.30$. These calculations gave confinement energy levels of ~35 meV for the electrons, ~55 meV for the heavy holes, ~165 meV for the light holes, and ~75 meV for the spin-orbit-split-off holes (all for a quantum

number of $n=1$).

From these results, we can finally obtain the 2D steplike-edge energies to be $E_{sh}^{2d}\sim 2.84$ eV for the hh-e transitions, $E_{sl}^{2D}\sim 3.09$ eV for the lh-e transitions, and $E_{ss}^{2D}\sim 3.42$ eV for the so-e transitions. The experimentally determined E_{sl}^{2D} and E_{ss}^{2D} values are, respectively, ~ 3.08 and ~ 3.35 eV. The agreement is found to be quite good in view of the uncertain parameter values[18] used. The $(E_0+\Delta_0)$-exciton Rydberg energy determined in the bulk ZnSe is ~ 40 meV [see Fig. 3(a)] which is about twice larger than the bulk E_0-exciton one.[19] The $(E_0+\Delta_0)$-exciton Rydberg energy in the SLS is also found to be 160 meV. In the exact 2D case, the 2D Rydberg value should be given by $G^{2D}=4G^{3D}$. We find that the present data agree well with this sample consideration. Such large values of the Rydberg energy in both bulk-ZnSe and ZnSe/ZnS SLS's, compared with those in the bulk-GaAs and GaAs/$Al_{1-x}Ga_xAs$ quantum wells, seem to be due to a smaller value of the dielectric constant for ZnSe (ZnSe and ZnS) than for GaAs (GaAs and $Al_{1-x}Ga_xAs$).[20]

IV. CONCLUSIONS

In conclusion, we have found the so-related steplike absorption edge and corresponding 2D exciton peak in the dielectric-function spectra of ZnSe/ZnS SLS's. The Rydberg value of this exciton is about 160 meV, which is 4 times larger than that of the bulk ZnSe. Theoretical calculations of the steplike-edge energies, based on the model-solid approach and Kronig-Penney model, were also performed and are found to agree well with the experimental observations. As we have paid no attention to valence-band mass anisotropy (the heavy-and light-hole masses and the resultant in-plane and z-direction masses) and ignored band nonparabolicity and valence-band coupling, it remains for future work to clarify their effects on the quantum energy levels, exciton Rydberg energies, etc.

[1] C. Weisbuch, in *Semiconductors and Semimetals,* edited by R. Dingle (Academic, New York, 1987), Vol. 24, p. 1.

[2] G. C. Osbourn *et al.*, in *Semiconductors and Semimetals* (Ref. 1), Vol. 24, p. 459.

[3] E. E. Mendez, L. L. Chang, G. Landgren, R. Ludeke, L. Esaki, and F. H. Pollak, Phys. Rev. Lett. **46**, 1230 (1981).

[4] G. Duggan, H. I. Ralph, P. Dawson, K. J. Moore, C. T. B. Foxon, R. J. Nicholas, J. Singleton, and D. C. Rogers, Phys. Rev. B **35**, 7784 (1987).

[5] M. Garriga, M. Cardona, N. E. Christensen, P. Lautenschlager, T. Isu, and K. Ploog, Phys. Rev. B **36**, 3254 (1987).

[6] C. G. Van de Walle and R. M. Martin, Phys. Rev. B **35**, 8154 (1987).

[7] C. G. Van de Walle, Phys. Rev. B **39**, 1871 (1989).

[8] Y. Kawakami and T. Taguchi, J. Vac. Sci. Technol. B **7**, 789 (1989).

[9] Y. Kawakami, T. Taguchi, and A. Hiraki, Nucl. Instrum. Methods B **33**, 603 (1988).

[10] S. Adachi and T. Taguchi, Phys. Rev. B **43**, 9569 (1991).

[11] T. Taguchi, I. Kidoguchi, and H. Nanba, U.S. Patent No. 4 866 007 (1989).

[12] S. Adachi, Phys. Rev. B **35**, 7454 (1987); **38**, 12 345 (1988); **38**, 12 966 (1988); **39**, 12 612 (1989); **41**, 1003 (1990); **41**, 3504 (1990).

[13] S. Adachi, J. Appl. Phys. **67**, 6427 (1990).

[14] T. Taguchi and Y. Yamada, in *Properties of II-VI Semiconductors,* MRS Symposia Proceedings No. 161 (Materials Research Society, Pittsburgh, 1990), p. 99.

[15] W. A. Harrison, J. Vac. Sci. Technol. **14**, 1016 (1977).

[16] K. Shahzad, D. J. Olego, and C. G. Van de Walle, Phys. Rev. B **38**, 1417 (1988).

[17] P. Lawaetz, Phys. Rev. B **4**, 3460 (1971). We obtained the heavy- and light-hole masses from $m_{hh}/m_0=(\gamma_1-2\gamma_2)^{-1}$ and $m_{lh}/m_0=(\gamma_1+2\gamma_2)^{-1}$, respectively, where γ_1 $(=3.77)$ and γ_2 $(=1.24)$ are the Luttinger parameters.

[18] We must note that there is no strong consensus in the literature as to the correct values for the deformation potentials and effective masses is semiconductors (and particularly in ZnSe and ZnS).

[19] H. Venghaus, Phys. Rev. B **19**, 3071 (1979).

[20] We note that the exciton Rydberg energy G^{3D} could be given by the equation $G^{3D}=\mu e^4/2\hbar^2\epsilon_s^2$, where μ is the exciton reduced mass and ϵ_s is the dielectric constant.